Int. J. Heat Mass Transfer. Vol. 15, pp. 1297–1315. Pergamon Press 1972. Printed in Great Britain

HEAT TRANSFER TO LIQUID DROPS FROM A SMALL DIAMETER CHANNEL AT TEMPERATURES IN THE FILM BOILING RANGE

J. J. HEBERT

Department of Mechanical and Aerospace, Engineering and Materials Science, Rice University, Houston, Texas 77001, U.S.A.

and

D. C. PRICE

Thermal and Fluid Sciences Center, Institute of Technology, Southern Methodist University, Dallas, Texas 75222, U.S.A.

(*Received* 6 *July* 1971 *and in revised form* 18 *October* 1971)

Abstract—An experimental study to determine the values of heat transfer per drop for small drops of water, methanol, and acetone falling down a heated channel of small diameter. Channel temperatures ranged from 118°K to 269°K above saturation, and channel diameters were smaller than drop diameters. Values of heat transfer per drop exhibited a maximum at a saturation excess of approximately 200°K for all three fluids. The occurrence of a maximum is assumed to be due to the effect of vapor viscosity on the growth of the vapor film. The occurrence of the maxima at a common value of saturation temperature excess is thought to occur because of the effect of vapor thermal conductivity, vapor density, modified heat of vaporization, and vapor viscosity on the rate of growth of the vapor film.

It was also found that heat transfer per drop is independent of channel length. High-speed motion pictures and visual observations lead to the assumption that all appreciable heat transfer takes place in a very short period of time after the drop first contacts the channel.

The maximum values of heat transfer per drop were found to be related to fluid properties, drop impact velocity, and geometry by the following relationship:

$$\frac{(Q_D)_{\max}(d/D)^{3\cdot088}}{d^3\lambda_{VF}\rho_L} = 0\cdot232\,(N_\sigma)^{0\cdot256}\,(N_\mu)^{-1\cdot632}\,(N_\rho)^{-2\cdot264}\,(We)^{0\cdot245}.$$

NOMENCLATURE

A, area [m^2];
c_p, specific heat at constant pressure; [J/kg°K];
d, drop diameter [m];
d', $d(D_{\max}/D)$, normalized drop diameter [m];
$D_{\max}$, reference channel diameter [m];
f, drop frequency [drops/min];
g_c, constant of proportionality in Newton's Second Law [1 kgm/Ns^2];
h, heat transfer coefficient [W/m^2°K]; height [m];
h_{fg}, enthalpy of evaporation [J/kg];
J, conversion factor [1 Nm/J];
k, thermal conductivity [W/m°K];
L, channel length [m];
M, mass [kg];
$\dot{m}$, mass rate of flow [kg/s];
n, width of ring of vapor film [m];
N_μ, $\dfrac{\mu_{VF}^2 g_c}{d'^2\lambda_{VF}J\rho_{VF}^2} \times 10^{11}$ [dimensionless];
N_ρ, $\dfrac{\rho_{VF}}{\rho_L} \times 10^3$ [dimensionless];
N_σ, $\dfrac{\sigma_L}{d'\lambda_{VF}\rho_L J} \times 10^8$ [dimensionless];

P, heater power consumption [W];
q, instantaneous heat transfer rate [W];
Q, heat transfer [J];
Q_D, heat transfer per drop [J];
t, time [s];
T, temperature [°K];
ΔT_x, $(T_s - T_f)$, saturation temperature excess of test surface [°K];
v, drop impact velocity [m/s];
v_{in}, velocity of vapor entering the vapor film [m/s];
W, velocity of vapor leaving the vapor film [m/s];
W_e, $\frac{\sigma_L g_c}{d' \rho_L v^2}$, modified Weber number [dimensionless].

Greek letters

δ, thickness of vapor film [m];
λ_{VF}, $h_{fg} + c_{pV}[(T_s - T_f)/2]$, modified heat of vaporization [J/kg];
μ, dynamic viscosity [Ns/m^2];
ρ, density [kg/m^3];
σ, surface tension [N/m];
τ, critical time [s]; shear stress [N/m^2].

Subscripts

D, drop;
f, saturation;
F, evaluated at film temperature; $T_f = (T_s + T_f)/2$;
L, liquid; electrical load;
max, maximum;
s, channel surface;
V, vapor.

INTRODUCTION

PROBLEMS related to controlling the temperature of a heated surface are met with in many industrial applications. In certain situations, such as a heat exchanger used in a nuclear power plant, the temperatures are relatively high: and the heat fluxes desired are also rather high. One technique which has the ability to maintain high values of heat flux is boiling heat transfer. However, nucleate boiling, with heat fluxes in the range of 10^6W/m^2, is limited to a narrow range of temperatures.

Above some critical temperature, called the burnout temperature, the liquid will be in the film boiling regime, and steady-state heat flux drops drastically.

A droplet in steady-state film boiling above a hot surface is said to be in the spheroidal or Leidenfrost state [1]. When a drop (or extended body) of liquid is in the Leidenfrost state, the temperature difference between surface and liquid is on the order of 140°K. The thickness of the vapor film is on the order of 0·1 mm; therefore, a temperature gradient as large as 1400°K/mm can exist in a stable situation.

Modern research into droplet film boiling heat transfer can be divided into two areas. The first involves research into the characteristics of steady-state Leidenfrost boiling of drops and extended masses. Heat fluxes achieved in such a situation are on the order of 10^4W/m^2. Publications dealing with such research done through March, 1967 are summarized by Bell [2]. The second area is research whose primary aim is to investigate those parameters which will lead to heat fluxes higher than 10^4 W/m^2. In general this second area will not encompass true film boiling, but the surface temperatures used are high enough to be considered in the film boiling regime.

In the present investigation, for example, the energy absorbed by the drops was the energy needed to start film boiling. not the energy required for steady-state film boiling. The measurements made during the course of this investigation were those of an end effect of the Leidenfrost phenomenon. After a drop strikes the heated surface it absorbs energy at a high rate while the vapor film is being formed: Then what is left of the drop vacates the heat transfer surface on a film of vapor so that the next drop can repeat the process.

In general, research into increasing the heat flux has been pointed toward decreasing the thickness of the vapor film, or causing direct contact between the liquid and hot surface.

Bradfield [3] reported on instances of contact during film boiling of drops. It was determined that contact could be induced by bouncing, surface roughnesses, or force fields. Later, Aylor and Bradfield [4] investigated the effects of electrostatic force upon droplet evaporation rate. It was found that electrostatic force increased the heat transfer rate only about 7 per cent.

Another attempt to increase heat flux was to cause the heating surface to move relative to the drop in steady-state film boiling. Experimental and analytical analyses relative to this were reported by Baumeister and Schoessow [5]. Using their analytical results, which match their experimental data closely, it was found that the average power to a drop of 4·42 mm i.d., moving 4·6 m/s relative to a heated surface, was approximately 2 W. For the present study a drop of the same initial diameter, moving down the channel with a relative velocity of approximately 1·2 m/s, draws power conservatively estimated at 2050 W. The tremendous difference between these two results arises because that of Baumeister and Schoessow [5] is for steady-state film boiling, whereas the present study is not.

Splattering of drops has been investigated, and it has proven to be a much more effective method of heat transfer than steady-state Leidenfrost boiling of liquid moving relative to a heated surface. Wachters and Westerling [6] studied heat transfer from a heated, inclined wall to impinging water drops; and Wachters, Smulders, Vermeulen and Kleiweg [7] studied heat transfer from a heated, inclined wall to impinging mist droplets. The water drops of [6] were approximately 2 mm dia., and the mist droplets of [7] were much smaller, but their behavior was found to be essentially the same. Both dynamics and heat transfer were studied by the investigators, with the emphasis on dynamics. Enough heat transfer data were gathered to discover that in one temperature region the heat transfer decreased with increasing temperature. The authors, however, neglected to identify this region.

A publication by McGinnis and Holman [8] dealt with individual droplet heat transfer rates for splattering. Heat transfer per drop was investigated, with little emphasis on dynamics. As much as 50 per cent of the theoretical maximum possible heat transfer was obtained during a single impact and rebound of a drop, for an impact velocity of about 3·7 m/s. The heat flux during impact and rebound was estimated at 10^9 W/m^2, a considerable improvement over steady-state Leidenfrost boiling. The region of temperature for which heat transfer per drop decreased with increasing temperature was also identified. This was seen to occur for saturation temperature excesses above about 167°K, for water, ethanol and acetone. At about this temperature excess a maximum in the heat transfer per drop occurred. An empirical correlation was obtained which related this maximum value of heat transfer per drop to drop diameter, impact velocity, and fluid properties.

It is believed that the high heat fluxes which are possible for small drops of liquid in Leidenfrost boiling can be obtained by containing the drop and causing the vapor film to partially or totally disperse. A small channel used as the heat transfer surface should accomplish these objectives; specifically, a channel whose diameter is smaller than the drop diameters to be studied.

The specific objectives of this experimental investigation are:

(1) To obtain values of heat transfer per drop as a function of test surface saturation temperature excess, drop frequency, drop diameter, channel length, channel diameter, drop impact velocity, and fluid. The fluids chosen were water, methanol, and acetone.

(2) To obtain an engineering correlation between the maximum values of heat transfer per drop, fluid properties, drop impact velocity, and pertinent geometries.

(3) To develop a physical description of the processes governing heat transfer per drop and its variation with the above-named parameters;

and to develop a comprehensive theory to explain the results obtained.

EXPERIMENTAL APPARATUS AND METHOD

Drops were generated by fluid flowing from a reservoir of fixed head through the tip of a hypodermic needle. A Nupro fine-metering needle valve was used to control the drop frequency. A plug valve, used only for on-off operation, was also placed in the line. The reservoir was operated at fixed head by continuously feeding fluid to it, and allowing the excess fluid to overflow through a notch in the rim of the reservoir. In the case of water, a scavenge pump was used to circulate overflow liquid back to the reservoir. However, for flammable liquids the scavenge pump motor would have been a fire hazard, and a second reservoir of yet higher head was used to supply the main reservoir.

The hypodermic needles used were one each of gauges 13, 15, 16, 18 and 22. Using the appropriate needle valve settings and needles, the drop frequency could be varied from 100 to 900 drops per min, and drop diameters from 2·54 mm to 4·32 mm could be obtained.

It was necessary to calibrate each needle with each fluid in order to determine how drop diameter varied with drop frequency. For a typical drop calibration point a large number of drops were collected at a known drop frequency, and the time required to collect them was recorded. A Strobotac was used to determine drop frequency. Using the Strobotac reading and the time, the total number of drops collected was calculated. The collected liquid was weighed on a precision balance, and the mass of each drop was calculated. With the assumption that each drop collected was spherical, the average diameter of each drop was calculated. The error in drop frequency was $\pm$ 1·3 per cent (due to the Strobotac), and the maximum error in drop diameter was $\pm$ 1·0 per cent. The drop frequency could be maintained directly on its recorded value by proper monitoring and adjustment of the fine-metering needle valve.

The test liquids were:

1. Water: distilled. b.p. 373·1°K
2. Methanol: reagent. b.p. 337·6°K
3. Acetone: reagent, b.p. 329·6°K

The central part of each of the two test specimens was a copper cylinder, 25·4 mm dia., with a small channel drilled and reamed along its axis of rotation. Each specimen also had a collar of copper. which served to support the central cylinder and to shed liquid. Each specimen was plated on all surfaces with 0·025 mm of nickel, by the electroless nickel plating process. The purpose of the nickel plating was to reduce heat loss by radiation, and to prevent oxidation of the copper.

Specimen 1 had an overall length of 80·96 mm. The channel along its axis of rotation was 76·20 mm long and 3·53 mm dia., at operating tem-

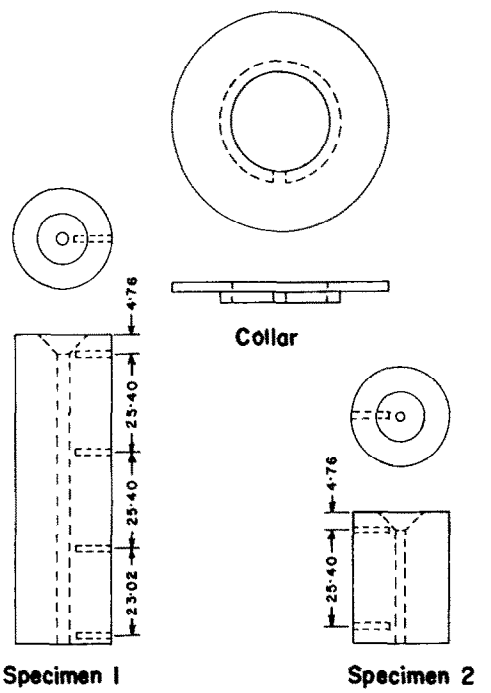

FIG. 1. Drawing of specimen 1, specimen 2, and a collar, showing location of thermocouple holes (dimensions in mm).

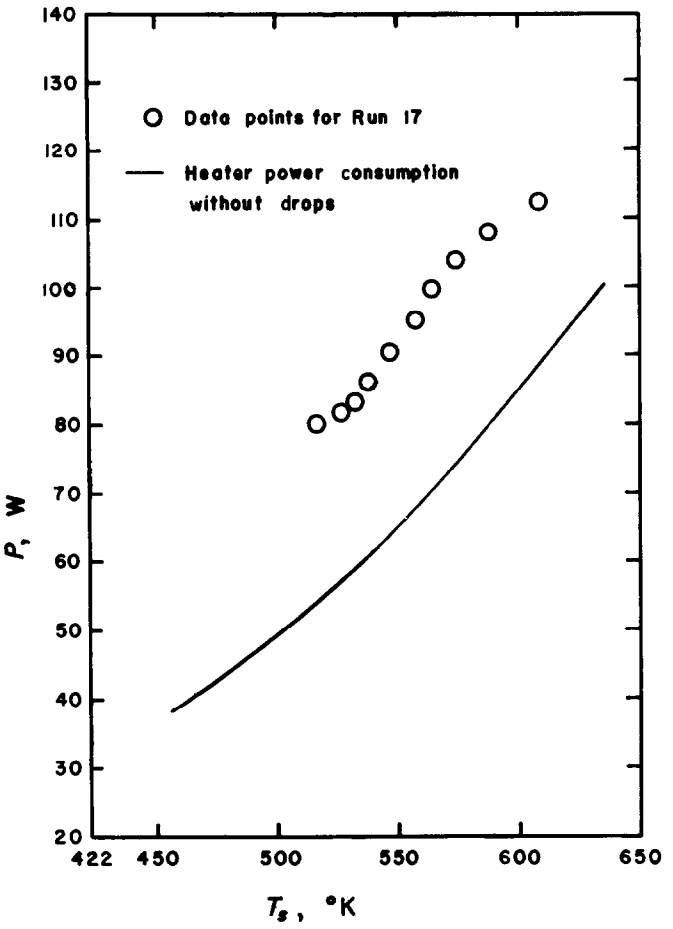

FIG. 2. Comparison between heater power consumption without drops and power consumption with drops (Run 17: Water drops; $d = 4{\cdot}42$ mm, $D = 3{\cdot}53$ mm, $f = 190$ drops per min).

perature. The remaining length of 4·76 mm was a 45° beveled entrance section. It was instrumented with four 30-gauge iron–constantan thermocouples installed 1·59 mm from the channel surface. The overall length of specimen 2 was 34·92 mm and the channel length was 30·16 mm. Channel diameter was 2·51 mm. It had two 30-gauge iron–constantan thermocouples installed 1·59 mm from the channel surface. Figure 1 is a drawing of both specimens and a collar, showing the location of thermocouple holes. Distances are in mm.

Specimen 1 was used with water as the only heat transfer fluid, and specimen 2 was used with water, methanol, and acetone.

The specimens were constructed as two separate units, each consisting of a cylinder, press-fitted collar, resistance heating wire, and the appropriate number of thermocouples. The resistance heating wire was 1·2 m of 30-gauge Chromel wire, with about 12 cm of 16-gauge nickel wire mechanically joined to each end for a power lead. The overall electrical resistance of this combination was about 25Ω. The heating wire was wrapped evenly around the cylinder so that each nickel lead made about one wrap,

and the Chromel wire was evenly distributed along the cylinder. Sauereisen cement was used to electrically insulate the specimen from the heating wire, and to hold the heating wire in place. Sauereisen cement was also used to install the thermocouples.

A cylindrical ceramic sleeve held the unit during calibration and data-taking procedures. The collars were made so that the shoulder of each collar fit snugly inside the ceramic sleeve, and the edge of each collar overlapped the sleeve approximately 3 mm. Thus the collar transferred the weight of the test specimen to the ceramic sleeve, which in turn was held in the proper position by a laboratory clamp.

Alternating current power supply to the specimen was controlled by a Powerstat variable transformer, and measured by an a.c. wattmeter accurate to $\pm 0{\cdot}5$ W. The thermocouple temperatures were recorded directly by a 6-channel recording potentiometer, accurate to $\pm 0{\cdot}25$ per cent of full scale (272–800°K). A ventilation system was used to prevent the occurrence of toxic and explosive vapor conditions when methanol or acetone were being tested.

The most important data desired from this investigation were values of the heat transfer per drop. The method used to obtain these values is conceptually very simple. First, for a given test specimen, a curve of heater power consumption as a function of the test surface temperature was obtained with no liquid drops involved. This represented all the heat losses due to the relationship of the specimen to its surroundings. The ventilation system was operated during the calibration of specimen 2.

After this information was obtained, another curve of heater power consumption versus surface temperature was obtained. This time droplets of a known diameter, frequency, and substance were used. Figure 2 features typical examples of the two curves mentioned here.

For each point enough data were gathered to compute heat transfer per drop. Additional data were also obtained in order to fully study the phenomena under investigation.

With the data thus obtained the assumption was made that. for any given surface temperature. the difference in heater power consumption as represented by the two values P_D and P_L was the power consumed by the liquid drops. The power thus obtained is the energy per unit time consumed by the steady stream of droplets. Energy per drop (heat transfer per drop) can be obtained by dividing this power difference by the drop frequency.

Thus, the heat transfer per drop, Q_D, may be shown to be:

$$Q_D = \frac{(P_D - P_L)}{(f)}. \tag{1}$$

RESULTS AND DISCUSSION

This investigation yielded sufficient data to allow conclusions to be made regarding the effects of drop frequency, drop diameter, channel length, surface temperature, drop impact velocity, and fluid upon the heat transfer from channel to drop. In addition, it was possible to obtain an engineering correlation between the heat transfer per drop, the fluid properties, drop impact velocity, and pertinent geometry.

The ranges of experimental conditions are given in Table 1.

Table 1. Ranges of experimental conditions for the substances investigated

Substance	d (mm)	v (m/s)	D (mm)	L (mm)
Water	3·56–4·42	0·869–1·301	3·53	76·20
	2·79–3·56	0·884	2·51	30·23
Methanol	2·82–3·33	0·884	2·51	30·23
Acetone	2·84–3·35	0·884	2·51	30·23

A data point consisted of a value of the heat transfer per drop, Q_D, and a corresponding value of the saturation temperature excess of the test surface, ΔT_x. An experimental run consisted of a series of data points taken with a particular drop frequency, drop diameter, drop impact

velocity, and test specimen. A change in one or more of these parameters constituted the establishment of a different run. Within each run the data points, between 3 and 20 in number, were obtained for different surface temperatures. A total of 21 different runs were made: 12 with water, 5 with methanol, and 4 with acetone. Of these, 19 runs yielded a maximum value of the heat transfer per drop, $(Q_D)_{max}$.

water at 196°K, the average for methanol at 197°K, and the average for acetone at 207°K. The minimum points occurred at saturation temperature excesses of about 153°K. The other 4 maxima are discussed within the context of the effects of velocity upon heat transfer per drop.

The effect of drop frequency on the values of heat transfer per drop can also be seen in Fig. 3.

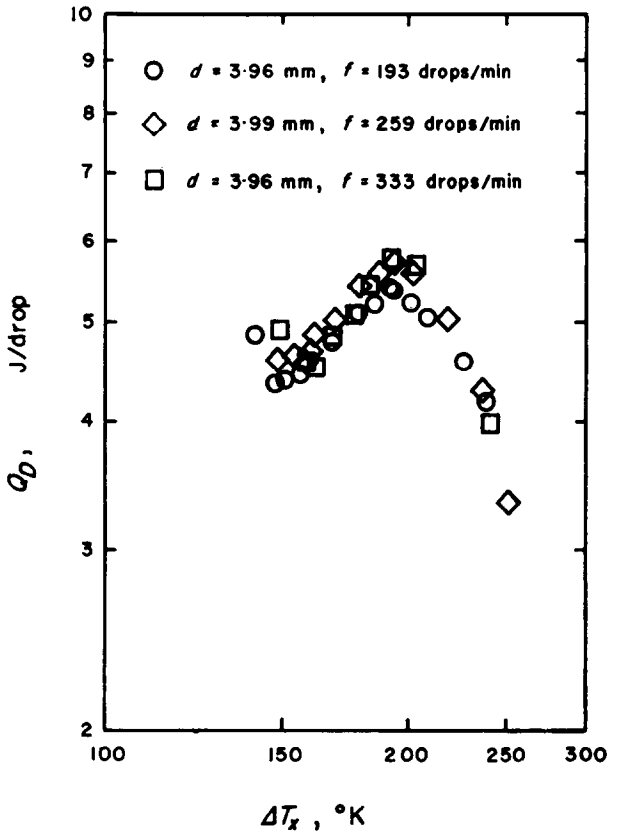

FIG. 3. Effect of drop frequency on the curve of heat transfer per drop versus saturation temperature excess. Water drops; D = 3·53 mm.

A typical plot of heat transfer per drop as a function of saturation temperature excess has a maximum and a minimum, as exhibited by the three curves in Fig. 3. Among the maxima, 15 occurred at saturation temperature excesses between 192°K and 209°K with the average for

The drop diameters are approximately the same, but the drop frequencies are appreciably different. For any given saturation temperature excess the values of heat transfer per drop are within 10 per cent of each other. Data points far to the left seem to show greater scatter, but these

are the points to the left of the minimums for each of the three runs. The data for each run exhibit the typical relationship between heat transfer per drop and saturation temperature excess.

It was found, however, that as the drop frequency increases to larger values, heat transfer per drop is no longer independent of drop frequency. At a frequency of 500 drops per min, and a drop diameter of 3·30 mm, acetone was found to exhibit the same relationship between heat transfer per drop and saturation temperature excess as was shown in Fig. 3. At a frequency of 605 drops per min and approximately the same drop diameter, however, the relationship is essentially linear over the temperature range investigated, and the values of heat transfer per drop are significantly different between the two cases. Thus, heat transfer per drop may be assumed to be independent of drop frequency, within a certain range of frequencies, but there is obviously a limit to this assumption.

A total of 10 values of $(Q_D)_{max}$ were obtained for water drops with specimen 1, and two values for water drops with specimen 2. In addition, four values of $(Q_D)_{max}$ were obtained for methanol drops with specimen 2, and three values for acetone drops with specimen 2. For each of these groups of values of maximum heat transfer per drop, the value of this parameter is approximately proportional to the cube of drop diameter. This means that the maximum heat transfer per drop is approximately proportional to the mass available for evaporation, for any one fluid and channel diameter. There were two values of maximum heat transfer per drop which did not conform to this relation, however. For the two experimental runs in question, the diameter ratio, (d/D), had a value of 1·008. This means that the drop and channel came into contact only very slightly, and thus this is a limiting case. It was also observed that the values of $(Q_D)_{max}$ for water were approximately one order of magnitude higher than those for methanol and acetone, and that the values for the latter two substances were approximately equal.

Two experimental runs were made with water at a drop diameter of 3·56 mm and a drop frequency of 195 drops per min: one with specimen 1 (D = 3·53 mm), and one with specimen 2 (D = 2·51 mm). The values of heat transfer per drop obtained with the smaller channel diameter were roughly double those obtained with the large diameter. Thus heat transfer per drop increases with increasing drop diameter, and decreases with increasing channel diameter. Expressing it another way, heat transfer per drop has been shown to increase with the ratio (d/D).

It became apparent during observations with specimens 1 and 2 that all appreciable heat transfer occurred while a drop was at or near the beginning of the channel. Thus, it is assumed that unless the channel were very short or very long, the length should have no measurable effect on the heat transfer per drop. Since this assumption is so crucial to correlation of the data and to a physical description of this study, it was decided to prove its validity experimentally.

Given two channels of different diameters, and test conditions similar in all ways, one should observe the evaporation of equal percentages of fluid for equal values of saturation temperature excess for two separate runs. The experiment which was used to validate the above assumption consisted of making two separate runs, with similar test conditions in the two runs for all parameters except channel length. To establish similar conditions the values of the parameter (d/D) were set as nearly equal as possible for the two runs; however, the length of specimen 1 was 76·45 mm and the length of specimen 2 was 30·23 mm. For complete dimensional similarity with specimen 1, specimen 2 was too short by a factor of about 1·7.

The results of the two runs are shown in Fig. 4. The ordinate is the ratio of actual heat transfer per drop, to the heat transfer required to completely evaporate a drop and raise its temperature to the film temperature. This is a measure of the percentage of the fluid which was

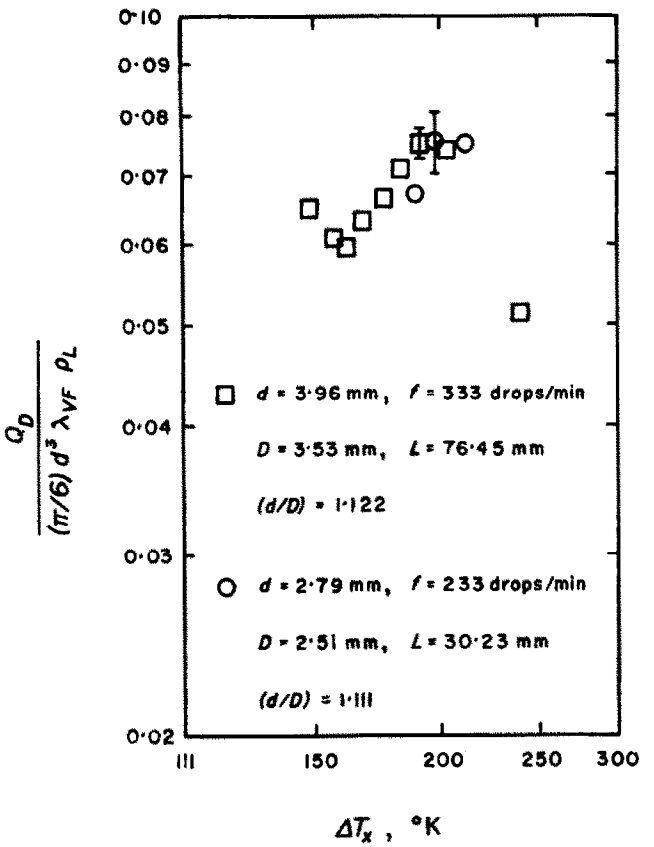

FIG. 4. Effect of channel length on the curve of the percentage of liquid evaporated vs. saturation temperature excess. Water drops.

evaporated. The abscissa is saturation temperature excess. The two vertical bars indicate the limits of uncertainty for their respective data points, as determined by the methods of [9]. One can readily see from Fig. 4 that the ordinates are nearly equal for comparable values of saturation temperature excess. Thus it is possible to make the conclusion that, for the channel lengths investigated, heat transfer per drop is independent of channel length.

Four experimental runs were made with water and specimen 1 to determine the effect of drop impact velocity on heat transfer per drop. Drop impact velocity is defined as the velocity with which the drop first contacts the channel. Values of drop impact velocity were calculated by assuming free-fall under the influence of gravity alone.

It can be seen in Fig. 5 that maximum heat transfer per drop is approximately proportional to drop impact velocity to the $-0{\cdot}6$ power, for velocities between 0·871 m/s and 1·301 m/s.

It has been shown that heat transfer per drop is independent of channel length, for the channel lengths investigated. One reason heat transfer per drop decreases with increasing drop impact velocity is that a high-velocity drop goes past this region of high heat transfer faster than a low-velocity drop. Another reason is that velocity gradients in the vapor film will be larger, and the resultant larger shear stress will retard dispersion of the vapor film.

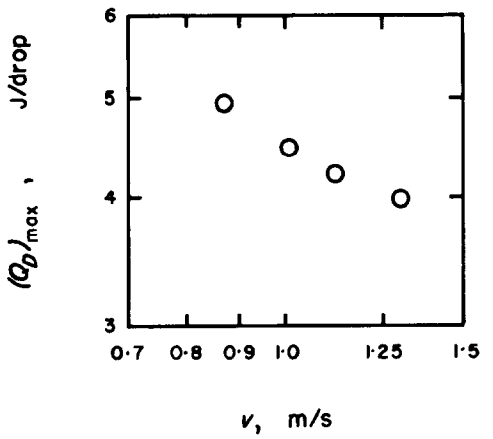

FIG. 5. Effect of drop impact velocity on maximum values of heat transfer per drop. Water drops; $d = 3{\cdot}99$ mm, $D = 3{\cdot}53$ mm, $f = 259$ drops per min.

Maximum values of heat transfer obtained during the velocity-variation runs exhibited two interesting anomalies, when compared to the other eight values of $(Q_D)_{max}$ obtained with water. The values of $(Q_D)_{max}$ for the former were about 13 per cent lower than expected, and the average saturation temperature excess was 11°K higher than expected. These anomalies are due to the fact that velocity-variation data were obtained approximately 10 months after the rest of the data. During this time interval it is likely that the nickel coating of specimen 1 oxidized, and became thinner after the oxide was removed for data taking. Thus, the nickel coating of specimen 1 presented less thermal resistance for these last runs than the runs made 10 months before. Under this condition one would expect to see the anomalies described above.

Reasons why a low thermal resistance causes these anomalies are presented in a detailed discussion of the effect on heat transfer per drop of a thin coating of scale on the heat transfer surface; reported by Hebert [10]. Very briefly, a drop striking a thin insulator (such as a coating of scale) causes a large enough temperature depression in the scale so that the liquid adjacent to the surface is momentarily in the nucleate boiling regime. Since nucleate boiling yields high heat fluxes, the heat transfer per drop is relatively large. It was also found that maximum values of heat transfer per drop occurred at much lower values of saturation temperature excess when the surface had a thin coating of scale.

The nickel coating on specimen 1 which existed during the accumulation of velocity-variation data was thinner than for the data obtained 10 months previously; and it thus presented less thermal resistance. Thus, the maximum values of heat transfer per drop should be smaller in magnitude, and they should occur at a higher value of saturation temperature excess.

Since these anomalies exist, the four data points of Fig. 5 cannot be included with the other data in a general correlation. However. Fig. 5 does establish a functional relationship between heat transfer per drop and drop impact velocity.

It was decided to obtain an engineering correlation between geometry, fluid properties, drop impact velocity, and the maximum values of heat transfer per drop. The relevant geometrical properties have been shown to be drop diameter and channel diameter. Among fluid properties, liquid density and liquid surface tension are important because they determine the deformation of the droplet. The area of effective heat transfer is determined by these parameters. Vapor viscosity determines how fast the vapor film dissipates, and thus how long the droplet undergoes rapid evaporation. Vapor density determines the concentration of vapor immediately surrounding the heated surface. A high density creates an effective back pressure, and retards evaporation. Enthalpy of evaporation and vapor specific heat determine how much heat must be introduced into a drop to produce a given amount of vapor; that is, they determine the amount of heat which will be required to produce enough vapor to form an insulating film. Fluid thermal conductivity is not considered to be an important quantity for this correlation. It has been noted that heat transfer

to a drop took place very rapidly, just as the drop entered the channel. Thus, the amount of heat transfer would seem to depend more upon how much the drop deforms upon touching the channel than upon what happens after deformation. That is to say, heat transfer per drop would seem to depend more upon the dynamical properties of surface tension, viscosity, velocity, and density than upon the thermal property of thermal conductivity.

A similitude analysis yielded the following

$$\frac{(Q_D)_{\max}}{d^3\lambda_{VF}\rho_L} = K(d/D)^A (N_\sigma)^B (N_\mu)^C (N_\rho)^D (We)^E . \quad (2)$$

In the expression in equation (2) the quantity d' is a normalized drop diameter defined by:

$$d' = d(D_{\max} D) . \quad (3)$$

The value of $D_{\max}$ used in this correlation was 0·00353 m, which is the channel diameter of specimen 1. This normalization was done so that equation (2) would be valid for any channel diameter. The quantity λ_{VF} is a modified latent heat of vaporization. It is defined by the equation:

$$\lambda_{VF} = h_{fg} + (c_{PV})\left(\frac{T_s - T_j}{2}\right). \quad (4)$$

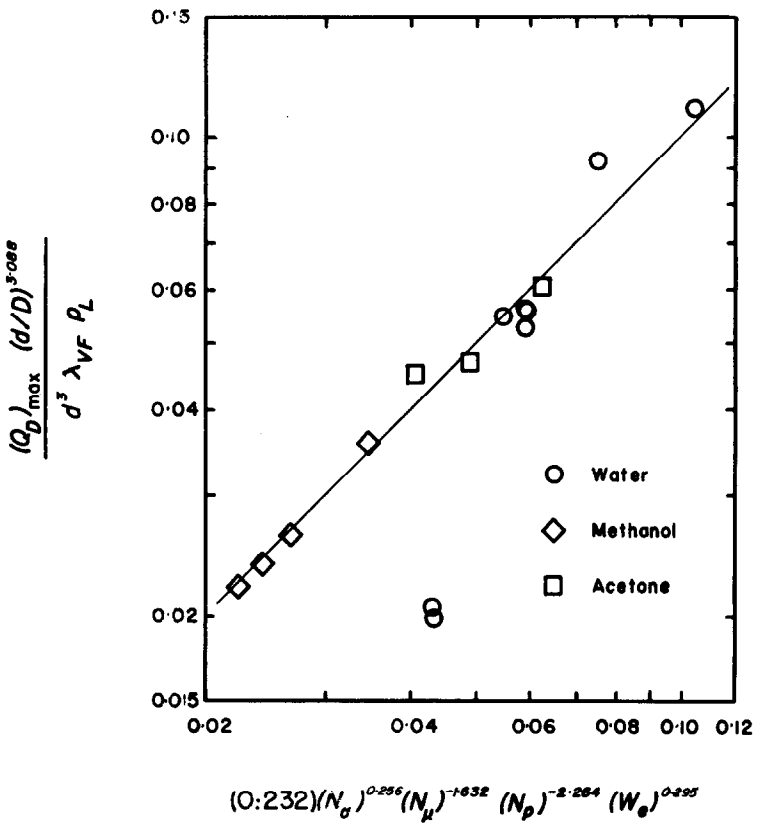

FIG. 6. Correlation of maximum values of heat transfer per drop.

It is the energy required to evaporate a unit mass of saturated liquid at atmospheric pressure, and superheat the vapor to the film temperature. It represents the energy content of vapor generated in film boiling, and is appropriate for this study. All other vapor properties were also evaluated at the film temperature, T_F. Liquid properties were evaluated at 293°K and one atmosphere pressure.

Thermophysical properties, obtained from [11–14], together with the 19 values of maximum heat transfer per drop, were used to solve for the constants in equation (2). The result is:

$$\frac{(Q_D)_{max}(d/D)^{3\cdot088}}{d^3\lambda_{VF}\rho_L} = (0\cdot232)(N_\sigma)^{0\cdot256}(N_\mu)^{-1\cdot632}(N_\rho)^{-2\cdot264} = (We)^{0\cdot295}. \quad (5)$$

Equation (5) is represented by the solid line in Fig. 6. It has a slope of 1·0, and the numerical values of ordinate and abscissa are equal everywhere along the line. It can be seen that equation (5) represents the data points well, except for the two points for which $(d/D) = 1\cdot008$. These two points are in the lower middle of Fig. 6. They represent the limiting case, that of very slight contact between drop and channel. For the other data points, the maximum deviation from the line is 16 per cent of the ordinate, and all others are less than 8 per cent.

Normalization with respect to saturation temperature excess was accomplished by plotting the quantity

$$\frac{Q_D}{(Q_D)_{max}}$$

as a function of ΔT_x, for each data point in the 13 runs used to obtain the peak value correlation of equation (5). Figure 7 shows the resultant

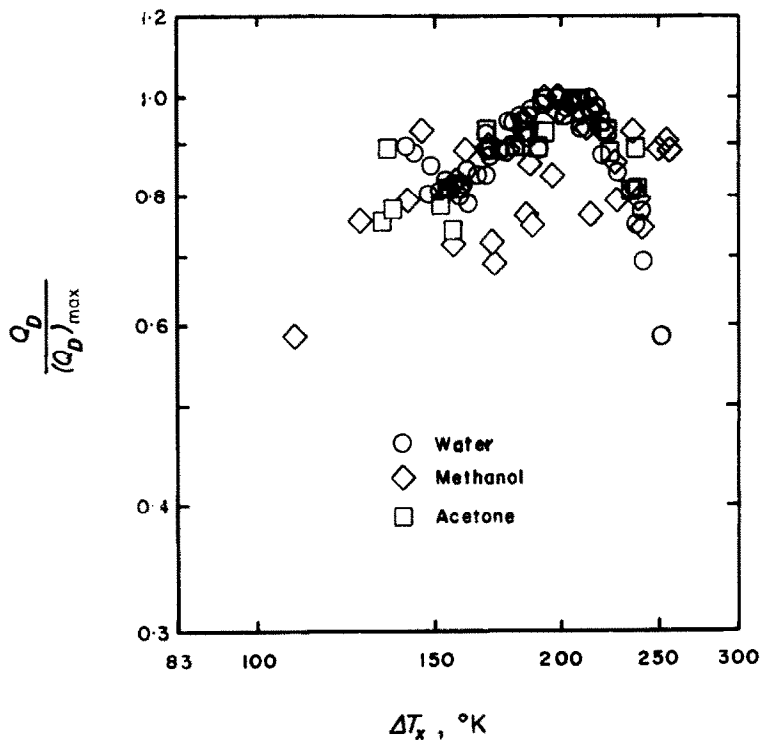

FIG. 7. Normalized data; heat transfer per drop vs. saturation temperature excess.

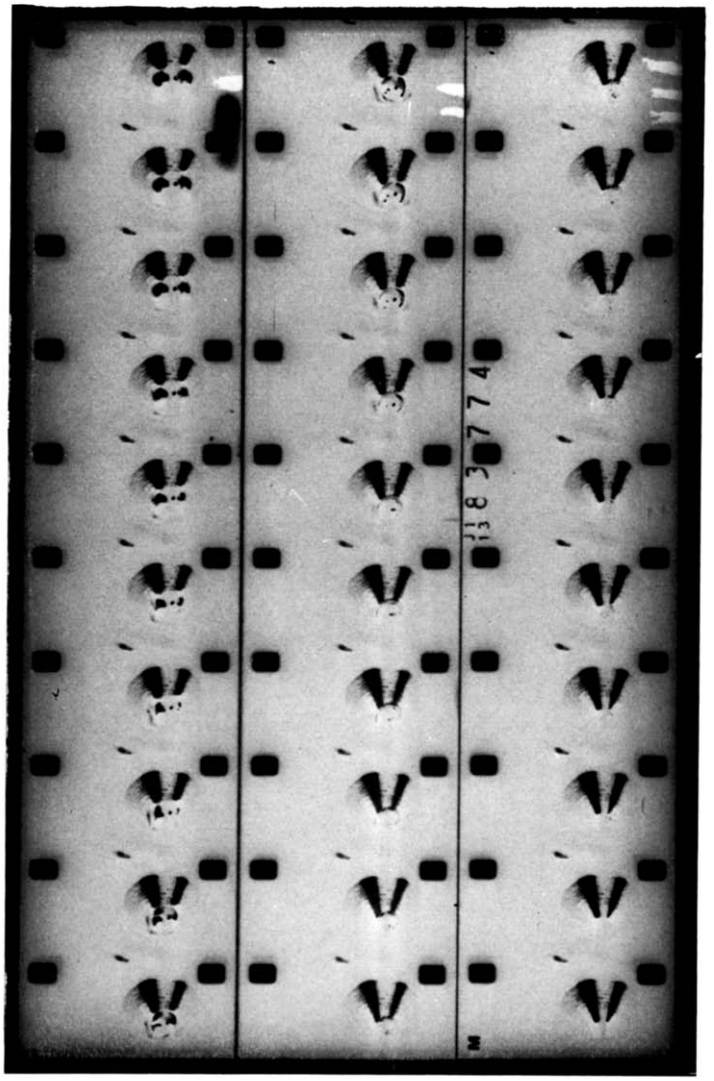

FIG. 8. Negative print of high-speed moving picture of drop interacting with heat-transfer surface (specimen 1). Frame rate is 3700 frames per second. Water drops; $d = 3{\cdot}89$ mm, $D = 3{\cdot}53$ mm, $f = 300$ drops per min, $T_s = 550°K$.

[*facing page* 1308]

plot. Note that the peak value is 1·0, at a saturation temperature excess of approximately 200°K. Normalization is quite good to the right of this peak value, with the exception of six data points. Scatter is more pronounced to the left of the peak value, particularly for the methanol data. There is no apparent trend to the scatter, so it is assumed that it arises due to uncertainties in the data. A total of 109 data points are included in Fig. 7, and about 20 can be said to deviate appreciably from the normalized curve.

PHYSICAL DESCRIPTION OF THE MECHANISM

Observations made during the course of this investigation make it possible to give a physical explanation of the trends in the data. Several attempts at an analytical solution were made, but all proved to be inadequate. The observations mentioned above showed that any simple mathematical model will disagree with experimental results by several orders of magnitude.

The sequence of interactions which take place when a drop of water receives heat from a channel is shown in Fig. 8. Figure 8 is a print of a high-speed movie film strip. It is printed in negative, and the viewer must keep in mind that actual dark and light areas are reversed in brightness. The two converging dark lines are actually strong reflections of light from the 45° beveled entrance section. The top opening of the channel is the small, light area at the bottom ends of the converging lines. The time interval between each frame is 0·00027 s.

Counting down from the top left hand side, the observer can see that the drop first makes contact at frame 9. The drop is slightly off center and the side away from the viewer touches first. Starting with frame 12 or 13, the drop deforms, and part of it appears to be sticking to the entrance region wall on the far side. The drop elongates due to this effect, but it never breaks apart. What was originally the topmost part of the drop disappears into the channel about frame 22, but the trailing part does not disappear until frame 30. In other words, that part of the drop which first touched the wall of the entrance section was retarded in movement, while the remainder of the drop continued its free-fall through the entrance region and into the channel. The drop did not separate, but elongated; and the trailing part was pulled into the channel after the main part of the drop.

As soon as part of a drop touches a hot surface, heat is transferred into the liquid, and vapor is formed. Some of the vapor forms an insulating film between the liquid and the hot surface, and some of it spreads into the surroundings. The trailing portion of the drop, that which touched first, effectively slides over the entrance section wall on a film of vapor. The viscosity of the vapor film causes this portion of the drop to lag behind the main body of the drop. This introduces a tumbling motion to the drop, and the tumbling motion will repeatedly expose relatively cool liquid, which is somewhat free of a vapor film, to the hot surface.

With each instance of contact, however, vapor will be released into the surroundings. After first contact and subsequent tumbling, the next contact will take place in an atmosphere which is somewhat saturated with vapor from the first contact. Heat transfer here will be inhibited. It is reasonable to assume that after a short interval of time the channel will be filled with vapor, and any heat transfer which takes place after this will be steady-state Leidenfrost boiling of liquid moving relative to a heated surface. The latter phenomenon has already been shown to yield very low heat transfer rates.

It is worthwhile to digress at this point to shed light upon one aspect of this investigation; the independence between heat transfer per drop and channel length. Heat transfer into the liquid takes place at a very fast rate, and it occurs at and near the entrance to the channel. After a drop has traveled a certain distance down the channel, enough vapor has been generated so that subsequent heat transfer is Leidenfrost boiling of liquid in motion relative to a heated surface.

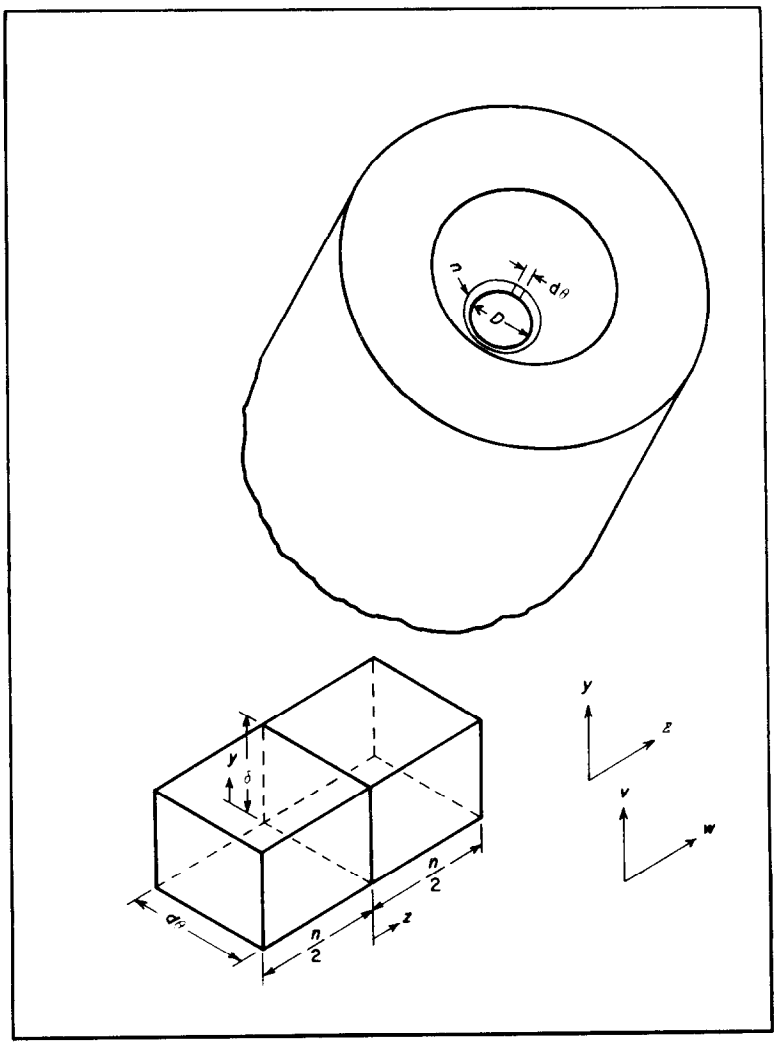

FIG. 9. Model for analysis of vapor layer.

Thus, unless the channel were very long, no appreciable heat transfer would take place beyond the point where this Leidenfrost boiling starts. Alternatively, for heat transfer to be independent of length, the channel must be at least long enough for the Leidenfrost state to become established before the drop leaves the channel.

Although attempts to obtain an accurate analytical solution for heat transfer per drop were futile, it was possible to develop a functional relationship between vapor film thickness and the parameters upon which it depends. The development is given in detail in Appendix A, and will be only briefly described here.

In Appendix A a model of a segment of the vapor film is described. The classical equations of Newton's Second Law of Motion, Conservation of Mass, and the First Law of Thermodynamics were applied to this model. After all

simplifying assumptions were made, four unknown variables were left: (1) vapor film thickness, δ, (2) contact area, πDn, (3) velocity of vapor leaving the film, W, and (4) time, t. It was possible to determine the relationship between vapor film thickness and time. This relation, developed in Appendix A, is given as:

$$\delta = \left[\frac{k_{VF}\Delta T_x t}{\rho_{VF}\lambda_{VF}} + \frac{4\mu_{VF}t}{\rho_{VF}}\right]^{\frac{1}{2}}. \qquad (6)$$

This equation, coupled with experimental results and observations, gives insight into the variation of heat transfer per drop with saturation temperature excess and with drop impact velocity.

The instantaneous rate of heat conduction across the vapor film can be approximated by:

$$q = k_{VF}(\pi Dn)\frac{\Delta T_x}{\delta} \qquad (7)$$

where πDn is the area of a ring representing the effective conduction area, as shown in Fig. 9. Equation (6) is an expression for δ in terms of known quantities and time, but equation (7) cannot be integrated to yield heat transfer per drop without first obtaining an expression for n in terms of known quantities and time.

It was not possible to obtain such an expression for the conditions of this investigation, but it is assumed that n is sensitive to drop impact velocity. It is reasonable to assume that this relationship will be of such a form that n increases with v. As n increases. more area is available for conduction, but the generated vapor must travel a greater distance to escape from beneath the drop. Since vapor viscosity will retard this motion, the vapor film will grow quickly, and the heat transfer per drop will decrease as drop impact velocity increases.

A typical curve showing the variation of heat transfer per drop with saturation temperature excess has a pronounced peak. The existence of this peak can be explained by considering the phenomena governing the growth of the vapor film. McGinnis and Holman [8], having integrated an expression such as equation (7), pointed out that the peaking occurred due to the opposing effects of thermal driving force (ΔT_x) and the critical contact time (τ), as they applied to growth of the vapor film.

As surface temperature increases, the thermal driving force causes the heat transfer to increase. This in turn causes vapor to be generated faster, at least initially. However, some of the vapor thus generated forms a film between the remaining liquid and the hot surface, and some of it dissipates into the surroundings.

For the fluids used in this investigation, vapor viscosity rises sharply with temperature. This indicates that as the surface temperature increases, resistance to the flow of the generated vapor increases. Thus there will be a critical temperature, at which the effect of increased rate of vapor generation will be offset by increased resistance to the movement of the vapor, and above which enough of the swiftly-generated vapor will stay between the remaining liquid and the hot surface to offset the effects of the increased thermal driving force. Above a certain value of saturation temperature excess, the critical contact time will be shortened by the action of vapor viscosity to such an extent that heat transfer per drop will decrease with increasing temperature.

Peaking of heat transfer per drop curves at a common value of saturation temperature excess was also reported by McGinnis and Holman [8], for water, ethanol, and acetone. It was attributed to the effect of the parameter ($k_{VF}/\rho_{VF}\lambda_{VF}$) on the growth of the vapor layer, and the fact that this parameter had the same value and thermal variation for the fluids tested. The values and thermal variations mentioned above are similar for the fluids used in the present investigation as well.

The results of the present investigation are shown by equations (5) and (6) to be affected by the action of vapor viscosity, as well as the thermal conductivity, density, and modified heat of vaporization of the vapor. Thus it is logical to assume that the location of the

maximum value of heat transfer per drop would depend upon vapor viscosity, as well as upon the parameter $(k_{VF}/\rho_{VF}\lambda_{VF})$. It has now been shown by [8] and by this study that, under identical experimental conditions, different fluids will exhibit maxima in heat transfer per drop at approximately the same saturation temperature excess.

CONCLUSIONS

1. The heat transfer per drop exhibits a definite maximum with respect to the saturation temperature excess of the test surface. This maximum occurred at a saturation temperature excess of approximately 200°K for all three fluids tested.

2. The occurrence of a maximum in the heat transfer per drop is a result of the effect of vapor viscosity on droplet contact time. As surface temperature increases, the increase in vapor viscosity retards dispersion of the generated steam, and allows more rapid buildup of an insulating vapor film.

3. The heat transfer per drop curves peak within a small range of values of saturation temperature excess, for all three fluids tested. The thermophysical properties which cause this are vapor thermal conductivity, vapor density, modified heat of vaporization, and vapor viscosity.

4. Heat transfer per drop is independent of channel length, for the channel lengths investigated in this study.

5. The maximum values of heat transfer per drop were found to be related to fluid properties, drop impact velocity, and geometry by equation (5). The experimental results agreed with this equation within 16 per cent. Curves of heat transfer per drop versus saturation temperature excess were normalized with good results by plotting the quantity $[Q_D/(Q_D)_{max}]$ as a function of saturation temperature excess.

6. The heat transfer received by the drops was the heat necessary to initiate film boiling. The amount of heat transfer per drop was rather small, but heat transfer rates as high as 2050 W were involved for short periods of time. Subsequent research is needed to find methods of extending this time period.

REFERENCES

1. T. B. Drew and A. C. Mueller, Boiling. *A.I.Ch.E. Trans.* **33**, 449–473 (1937).
2. K. J. Bell, The Leidenfrost phenomenon: A survey. *Chem. Enging Prog. Symp. Ser.* **63** (79), 73 (1966).
3. W. S. Bradfield, Liquid–solid contact in stable film boiling, *I/EC Fundamentals*, **5**, 200–204 (1966).
4. D. Aylor and W. S. Bradfield, Effects of electrostatic force, relative humidity, heating surface temperature, and size and shape on droplet evaporation rate. *I/EC Fundamentals* **8**, 8–16 (1969).
5. J. K. Baumeister and G. J. Schoessow, Creeping flow solution of Leidenfrost boiling with a moving surface. Tenth National ASME– AIChE Heat Transfer Conference, Philadelphia, Pennsylvania, 11–14 August (1968).
6. L. H. J. Wachters and N. A. J. Westerling, The heat transfer from a hot wall to impinging water drops in the spheroidal state. *Chem. Enging Sci.* **21**, 1047–1056 (1966).
7. L. H. J. Wachters, L. Smulders, J. R. Vermeulen and H. C. Klieweg, The heat transfer from a hot wall to impinging mist droplets in the spheroidal state. *Chem. Enging Sci.* **21**, 1231–1238 (1966).
8. F. K. McGinnis, III and J. P. Holman, Individual droplet heat-transfer rates for splattering on hot surfaces. *Int. J. Heat Mass Transfer* **12**, 95–108 (1969).
9. S. J. Kline and F. A. McClintock, Describing uncertainties in single sample experiments. *Mech. Enging* **75**, 3–8 (1953).
10. J. J. Hebert, An experimental investigation of heat transfer to liquid drops from a small diameter channel at temperatures in the film boiling range, Ph.D. Thesis, Southern Methodist University (1970).
11. D. D. Hodgman, (ed)., *Handbook of Chemistry and Physics*, 39th ed. Chemical Rubber Publishing Co, Cleveland, Ohio (1958).
12. O. P. Kharbanda, Thermal conductivity charts for gases, *Chem. Enging* **62** (7), 236 (1955).
13. N. A. Lange, (ed), *Handbook of Chemistry*, McGraw-Hill, New York (1967).
14. R. C. Weast, (ed), *Handbook of Chemistry and Physics*, 48th ed. The Chemical Rubber Co. Cleveland, Ohio (1967).
15. H. Lamb, *Hydrodynamics*, 6th ed. Dover Publications, New York (1945).

APPENDIX

Figure 9 is a sketch of the model used to analyze the vapor film in the context of this study. While heat is being transferred across the vapor film it is assumed that the effective

conduction area can be represented by a ring of area πDn, where n is time dependent. It is also assumed that vapor leaves this conduction area from both sides with average velocity W, which is also time dependent. The vapor layer thickness, δ, is assumed to be time dependent also. The classical equations of Newton's Second Law of Motion, Conservation of Mass, and the First Law of Thermodynamics are used to find a relationship between vapor layer thickness and time.

The following additional assumptions are made:

(1) Upon contact the drop will spread out while heat is being conducted into the liquid. The contact area is approximated by πDn; n varies with time, and n has some finite value when vapor begins to form.

(2) Vapor layer thickness does not vary with location.

(3) Vapor properties are constant throughout the vapor layer, and they are evaluated at the film temperature.

(4) Velocity in the z-direction, w, has a parabolic distribution with respect to y, has a linear distribution with respect to z, and has a value of zero at $z = 0$.

(5) Velocity in the y-direction, v, varies linearly between a maximum at $y = \delta$ and zero at $y = 0$.

(6) Velocity is zero in the θ-direction.

(7) A small segment of the conduction area ring can be approximated by a rectangle $d\theta$ wide and n long.

(8) Heat flux into the liquid across the vapor film can be approximated by:

$$Q/A = k_{VF}\Delta T_x/\delta . \tag{A.1}$$

The velocity distribution in the z-direction, at an arbitrary cross-section, will be:

$$w = \frac{4w_0}{\delta}y - \frac{4w_0}{\delta}y^2 , \tag{A.2}$$

where w_0 is the maximum velocity at the cross section; and:

$$w_0 = \frac{2W_0 z}{n} , \tag{A.3}$$

where W_0 is the maximum velocity at $z = n/2$.

Let us designate $\bar{w}$ the average w at an arbitrary cross-section, and W the average w at $z = n/2$. Then:

$$\bar{w} = \frac{2}{3}w_0 = \frac{2Wz}{n} ; \text{ and} \tag{A.4}$$

$$\left(\frac{\partial w}{\partial y}\right)_{\text{wall}} = -\left(\frac{\partial w}{\partial y}\right)_{\text{drop}} = \frac{12Wz}{\delta n} . \tag{A.5}$$

Newton's Second Law of Motion as applied to an incremental volume $(\delta d\theta dz)$:

$$-\tau_{\text{wall}}(d\theta dz) - \tau_{\text{drop}}(d\theta dz) = m\frac{d\bar{w}}{dt} + \bar{w}\frac{dm}{dt} \tag{A.6}$$

$$\tau_{\text{wall}} = \tau_{\text{drop}} = \mu_{VF}\left(\frac{\partial w}{\partial y}\right)_{\text{wall}} = \frac{12\mu_{VF}Wz}{\delta n} . \tag{A.7}$$

Equation (A.6) becomes:

$$\frac{-12\mu_{VF}}{\rho_{VF}\delta^2}(W/n) = \frac{d}{dt}(W/n) + \frac{k_{VF}\Delta T_x}{\rho_{VF}\lambda_{VF}\delta^2}(W/n) - 2(W/n)^2 . \tag{A.8}$$

This equation relates the time-dependent quantities W, n and δ to time. Two more such equations will be developed by applying Conservation of Mass and the First Law of Thermodynamics.

Conservation of Mass as applied to the entire volume:

$$\dot{m}_{\text{in}} - \dot{m}_{\text{out}} = \dot{m}_{\text{gain}} . \tag{A.9}$$

When the above quantities are evaluated equation (A.9) becomes:

$$\frac{k_{VF}\Delta T_x}{\rho_{VF}\lambda_{VF}} = 2\delta^2(W/n) + \frac{\delta}{n}\frac{d}{dt}(n\delta) . \tag{A.10}$$

The First Law of Thermodynamics as applied to the entire volume:

$$\dot{Q} + \dot{m}_{\text{in}}\left(h + \frac{v^2}{2} + z\right)_{\text{in}} = \dot{W} + \dot{m}_{\text{out}}\left(h + \frac{v^2}{2} + z\right)_{\text{out}} + \frac{d}{dt}\left(mu + \frac{v^2}{2} + z\right)_{\text{system}} . \tag{A.11}$$

The terms in equation (A.11) are to be evaluated according to the assumptions and the following equations:

$$v_{\text{in}} = (\dot{m}/\rho A)_{\text{in}} = \frac{k_{VF}\Delta T_x}{\rho_{VF}\lambda_{VF}\delta} \tag{A.12}$$

$$\dot{W} = P\frac{d}{dt}(\text{volume}) = \frac{Pd\theta}{2}\frac{d}{dt}(n\delta) . \tag{A.13}$$

$\dot{Q}$ is due solely to viscous dissipation, since all heat being transferred from surface to liquid is *across* the vapor film and not *to* it. Thus, from Lamb [15]:

$$\dot{Q} = \mu_{VF}\,d\theta\left\{\frac{n}{\delta}\left[\left(\frac{k_{VF}\Delta T_x}{\rho_{VF}\lambda_{VF}\delta}\right)^2 + 2W^2\right] + \frac{\delta}{n}\left(\frac{24W^2}{5}\right)\right\} . \tag{A.14}$$

All the terms of equation (A.11) have thus been accounted for. When these terms are substituted into equation (A.11), and the resultant equation has been simplified somewhat, the result is:

$$\frac{2\mu_{VF}}{\rho_{VF}\lambda_{VF}}\left(\frac{2\delta}{n}\right)\left[\frac{n}{\delta}(v^2_{\text{in}} + 2W^2) + \frac{24\delta W^2}{5n}\right] + \frac{k_{VF}\Delta T_x}{\rho_{VF}\lambda_{VF}} + \frac{\delta}{2\lambda_{VF}}v^3_{\text{in}} = 2\delta^2(W/n) + \frac{\delta}{n}\frac{d}{dt}(n\delta) + \frac{\delta^2 W^3}{n\lambda_{VF}} . \tag{A.15}$$

Equation (A.10) can be subtracted from equation (A.15) to yield:

$$\frac{2\mu_{VF}}{\rho_{VF}\lambda_{VF}}\left(\frac{2\delta}{n}\right)\left[\frac{n}{\delta}(v^2_{in}+2W^2)+\frac{24\delta W^2}{5n}\right]+\frac{\delta}{2\lambda_{VF}}v^3_{in}=\frac{\delta^2W^3}{n\lambda_{VF}}. \quad (A.16)$$

Dividing each term in equation (A.16) by (W^2/λ_{VF}) yields:

$$\frac{2\mu_{VF}}{\rho_{VF}}[(v_{in}/W)^2+2+\frac{24}{5}(\delta/n)^2]+\frac{\delta}{2}(v_{in}/W)^2(v_{in})=\delta^2(W/n). \quad (A.17)$$

Since n is some finite value when δ is starting from zero, the quantities $(v_{in}/W)^2$ and $(\delta/n)^2$ can be assumed to be very small numbers during the period of interest. If these quantities are assumed to be negligible, equation (A.17) simplifies to:

$$(W/n)=\frac{4\mu_{VF}}{\rho_{VF}\delta^2}. \quad (A.18)$$

When equation (A.18) is substituted into equation (A.8), the result is a differential equation involving δ and t only.

$$\frac{-12\mu_{VF}}{\rho_{VF}\delta^2}\left(\frac{4\mu_{VF}}{\rho_{VF}\delta^2}\right)=\frac{d}{dt}\left(\frac{4\mu_{VF}}{\rho_{VF}\delta^2}\right)+\frac{k_{VF}\Delta T_s}{\rho_{VF}\lambda_{VF}\delta^2}\left(\frac{4\mu_{VF}}{\rho_{VF}\delta^2}\right)-2\left(\frac{4\mu_{VF}}{\rho_{VF}\delta^2}\right)^2. \quad (A.19)$$

The variables can be separated in equation (A.19), and it can be integrated to yield an expression for vapor film thickness as a function of thermophysical properties, saturation temperature excess, and time. The result of this integration is

$$\delta=\left[\frac{k_{VF}\Delta T_s t}{\rho_{VF}\lambda_{VF}}+\frac{4\mu_{VF}t}{\rho_{VF}}\right]^{\frac{1}{2}}. \quad (A.20)$$

Thus, it can be seen that vapor film thickness is a function of vapor thermal conductivity, vapor density, modified heat of vaporization, and vapor viscosity; as well as saturation temperature excess and time.

TRANSFERT THERMIQUE À DES GOUTTES LIQUIDES PAR UN CONDUIT DE PETIT DIAMÈTRE À DES TEMPÉRATURES DANS LE DOMAINE DE L'ÉBULLITION EN FILM

Résumé—On détermine par une étude expérimentale les valeurs du transfert thermique à chaque goutte pour des petites gouttes d'eau, méthanol et acétone qui tombent dans un conduit chauffé et de faible diamètre. Les températures du conduit sont comprises entre 118°K et 269°K au-dessus de la saturation et les diamètres du conduit sont plus petits que la diamètre des gouttes. Les valeurs du transfert thermique à chaque goutte révèle un maximum pour un excès de 200°K par rapport à la température de saturation, ceci pour les trois fluides. L'occurence d'un maximum est supposée être due à l'effet de la viscosité de la vapeur sur la croissance du film de vapeur. L'existence des maximums à une valeur commune de l'excès de température par rapport à la saturation est reliée à l'effet sur la vitesse de croissance du film de vapeur de la conductivité thermique de la vapeur, de la masse volumique de la vapeur, de la chaleur latente de vaporisation et de la viscosité de la vapeur.

Il a été trouvé que le transfert thermique par goutte est indépendant de la longueur du conduit. Des vues à grande vitesse et des observations visuelles conduisent à l'idée que le transfert thermique se produit dans une très courte période de temps qui suit le premier contact entre la goutte et le conduit.

Les valeurs maximales du transfert thermique par goutte ont été trouvées reliées aux propriétés du fluide, à la vitesse d'impact de la goutte et à la géométrie par la relation suivante:

$$\frac{(Q_D)_{max}(d/D)^{3,088}}{d^3\lambda_{VF}\rho_L}=0{,}232(N_\sigma)^{0,256}(N_\mu)^{-1,632}(N_\rho)^{-2,264}(We)^{0,245}$$

WÄRMEÜBERGANG AN FLÜSSIGKEITSTROPFEN IN EINEM ENGEN KANAL BEI TEMPERATUREN IM FILMSIEDEBEREICH

Zusammenfassung—Der Wärmeübergang am Einzeltropfen wird experimentell bestimmt für kleine, frei fallende Tropfen von Wasser, Methanol und Azeton in einem beheizten Kanal kleinen Durchmessers. Die Kanaltemperatur betrug 118 K bis 269 K über Sättigungszustand, und die Kanaldurchmesser waren kleiner als die Tropfendurchmesser. Die Wärmeübergangswerte erreichten bei allen drei Flüssigkeiten ein Maximum bei einer Übertemperatur von etwa 200 K. Das Auftreten eines Maximums wird dem Einfluss der Dampfviskosität auf das Wachsen des Dampffilmes zugeschrieben. Die Maxima bei normalen Übertemperaturen werden den Einfluss der Wärmeleitfähigkeit des Dampfes, der Dampfdichte, der veränderlichen Verdampfungswärme, und der Dampfviskosität auf die Wachstumsrate des Dampffilmes zurückge-

Hochgeschwindigkeitsfilmaufnahmen und visuelle Beobachtungen führten zu der Annahme, dass der Hauptwärmeübergang in der sehr kurzen Zeitspanne erfolgt, nach der ersten Berührung des Tropfens mit dem Kanal.

Es wurde gefunden, dass die Maximalwerte für den Wärmeübergang von den Flüssigkeitseigenschaften, von der Tropfenauftreffgeschwindigkeit und von der Geometrie abhängen nach folgender Beziehung:

$$\frac{(Q_D)_{\max}(d/D)^{3,088}}{d^3\lambda_{VF}\cdot\rho_L} = 0{,}232\,(N_\sigma)^{0,256}(N_\mu)^{-1,632}(N_\rho)^{-2,264}(We)^{0,245}$$

ТЕПЛООБМЕН МЕЖДУ КАПЛЯМИ ЖИДКОСТИ И КАНАЛОМ МАЛОГО ДИАМЕТРА В ДИАПАЗОНЕ ТЕМПЕРАТУР ПЛЕНОЧНОГО КИПЕНИЯ

Аннотация—Экспериментально определялись значения коэффициента теплообмена для отдельных небольших капель воды, метанола и ацетона, падающих в нагретом канале малого диаметра. Температура канала, отсчитываемая от температуры насыщения, изменялась от 118°К до 269°К, а диаметры капель превышали диаметры канала. Для всех трех жидкостей значения коэффициента теплообмена капли были максимальными при температуре, примерно на 200°К превышающей температуру насыщения. Предполагается, что местоположение максимума является следствием влияния вязкости пара на рост пленки пара. Местоположение максимума коэффициента теплообмена при обычном превышении температуры насыщения объясняется влиянием теплопроводности, плотности и вязкости пара, а также скрытой теплоты парообразования на интенсивность роста пленки пара.

Найдено, что теплообмен капли не зависит от длины канала. Скоростная съёмка и визуальные наблюдения позволяют сделать предположение, что теплообмен в основном происходит в очень короткий промежуток времени сразу же после контакта капли с каналом. Получено следующее соотношение для описания зависимости между максимальными значениями теплообмена капли и свойствами жидкости, частотой падения капель и геометрической конфигурацией:

$$\frac{(Q_D)_{\max}(d/D)^{3,088}}{d^3\lambda_{VF}\rho_L} = 0{,}232(N_\sigma)^{0,256}(N_\mu)^{-1,632}(N_\rho)^{-2,264}(We)^{0,275}$$